

UNCLASSIFIED

AD 4 2 3 9 4 2

DEFENSE DOCUMENTATION CENTER

FOR

SCIENTIFIC AND TECHNICAL INFORMATION

CAMERON STATION, ALEXANDRIA, VIRGINIA



UNCLASSIFIED

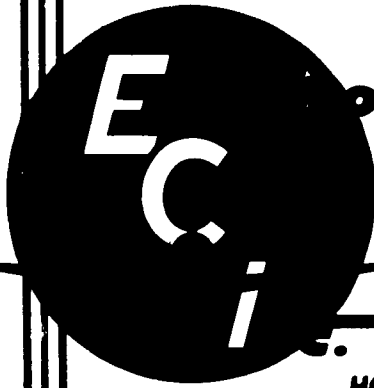
NOTICE: When government or other drawings, specifications or other data are used for any purpose other than in connection with a definitely related government procurement operation, the U. S. Government thereby incurs no responsibility, nor any obligation whatsoever; and the fact that the Government may have formulated, furnished, or in any way supplied the said drawings, specifications, or other data is not to be regarded by implication or otherwise as in any manner licensing the holder or any other person or corporation, or conveying any rights or permission to manufacture, use or sell any patented invention that may in any way be related thereto.

CATALOGED BY DDC

423942

AS AD NO.

Final Engineering Report
 for
PROTOTYPE HIGH POWER CIRCULATOR
 WITH
SOLID STATE LIMITER



ONIC
UNICATIONS

HOME OFFICE—ST. PETERSBURG, FLORIDA

RESEARCH DIVISION
1830 YORK ROAD
TIMONIUM, MARYLAND

NOV 28 1969
 TISIA B

UNCLASSIFIED

**Final Engineering Report
for
PROTOTYPE HIGH POWER CIRCULATOR
WITH
SOLID STATE LIMITER**

**This report covers the period
20 April 1962 to 30 June 1963**

**Electronic Communications, Inc.
Research Division
1830 York Road
Timonium, Maryland**

July 17, 1963

Navy Department

Bureau of Ships

Electronics Division

Contract No. NObsr-87394

Project Serial No. SF0010205 ST 6158

UNCLASSIFIED

ABSTRACT

A prototype high power Y-circulator with a solid state limiter has been constructed and tested as required by the specifications of this contract. The circulator package was delivered to the Chesapeake Bay Annex of the Naval Research Laboratory.

The power handling capability of the circulator is limited by the VSWR of the antenna used in the system. Any reflection of 10 Kw or more from the antenna will damage the solid state limiter connected to the receiver port.

A ferroelectric limiter has been designed and constructed for the purpose of replacing the limiter presently in the circulator package. The tests made on this device have been very satisfactory, as the data in this report will show.

TABLE OF CONTENTS

	<u>Page</u>
ABSTRACT	i
LIST OF ILLUSTRATIONS	iii
1. PURPOSE	1
2. GENERAL FACTUAL DATA	2
2.1 <u>Background</u>	2
2.2 <u>Measurement Procedures</u>	3
2.3 <u>References</u>	4
2.4 <u>Definition of Symbols</u>	4
2.5 <u>Identification of Technical Personnel</u>	4
2.6 <u>Patents</u>	4
3. DETAIL FACTUAL DATA	5
3.1 <u>Circulator Components</u>	5
3.2 <u>Ferroelectric Limiter</u>	6
3.3 <u>Properties of Ferroelectric Materials</u>	7
3.4 <u>Construction of Limiter</u>	8
3.5 <u>Principle of Operation</u>	9
3.6 <u>Temperature Rise and Thermal Relaxation</u>	14
3.7 <u>Measured Limiter Performance</u>	20
3.8 <u>Circulator Performance at Low Power</u>	23
3.9 <u>Circulator Performance at High Power</u>	23
4. CONCLUSION	25

LIST OF ILLUSTRATIONS

Page

- Figure 1 - High Voltage Test
- Figure 2 - Set Up For Low Power Measurement of Prototype Circulator
- Figure 3 - Measurement of Ferroelectric Properties
- Figure 4 - Set Up For Measurement of Recovery Time
- Figure 5 - Set Up For High Power Measurement of Prototype Circulator
- Figure 6 - Top View Photograph of High Power Y-Circulator
- Figure 7 - Characteristics of Micro-State Limiter
- Figure 8 - Dielectric Constant vs Temperature Characteristics of Ferroelectric Materials
- Figure 9 - Dielectric Constant vs DC Applied Voltage Characteristics of Ferroelectric Material UR 5324
- Figure 10 - Parallel Plane Waveguide Configuration
- Figure 11 - Frequency Response of Ferroelectric Loaded Cavity
- Figure 12 - Ferroelectric Limiter Configuration
- Figure 13 - Characteristics of Ferroelectric Limiter For Q_L of 47.5
- Figure 14 - Characteristics of Ferroelectric Limiter For Q_L of 28.3
- Figure 15 - Low Power Characteristics of Prototype Circulator
- Figure 16 - Oscilloscope Trace Photograph For Recovery Time Measurement
- Figure 17 - Oscilloscope Trace Photograph For Recovery Time Measurement
- Figure 18 - Oscilloscope Trace Photograph For Recovery Time Measurement

1. PURPOSE

Through the successful development of an experimental high power Y-Circulator⁽¹⁾ in the UHF region has come the need for a device more compatible in size to the equipment with which it will be used. The purpose of this contract was to modify the experimental model into a unit which could be mounted in a standard 19" relay rack. A solid state limiter was also to be supplied with the circulator package in order to give the maximum transmitter-receiver isolation possible. Emphasis was placed on compactness and simplicity of operation.

2. GENERAL FACTUAL DATA

2.1 Background

A high power Y-circulator for the UHF region was constructed and tested under a previous contract.⁽²⁾ This unit was an experimental model designed to measure the performance characteristics of a Y-circulator when subjected to high RF power levels. The circulator functioned normally under a peak power of approximately 1 megawatt and an average power of 2 kilowatts. These tests were performed at the Chesapeake Bay Annex of the Naval Research Laboratory. The experimental Y-circulator was then returned to this company for the purpose of constructing a prototype model as required by this contract.

A new ferrite disc enclosure was fabricated and fitted with 3-1/8" coaxial connectors on the transmitter and antenna ports. The receiver port is a type "HN" - UG 560 receptacle. Since the receiver side of the circulator will always be 20 db down from the transmitter side it was possible to use a type "HN" fitting. High voltage dc tests were performed to detect any possible breakdown paths in the new configuration. The circulator performance characteristics were measured under low RF power as a function of temperature. This measurement determines the exact temperature at which the ferrite discs must be kept in order to obtain maximum isolation for a given frequency and magnetic field.

A cooling system capable of keeping the ferrite discs at the proper temperature for maximum isolation for a cw power input of 2 kilowatts was obtained from Budd Electronics. This unit is model CRG-3033 and delivers 4.4 GPM of Freon 113 at 40 psig. Its maximum cooling capacity is 1880 BTUH which is enough to handle 550 watts of dissipation. The circulator presents a heat load of 200 watts at 2000 watts of cw power input.

The limiter supplied in the circulator package is a solid state device supplied by Micro-State Electronics. This unit is rated

at 10 kw peak power and 60 watts average power with an isolation greater than 40 db. The peak power rating of this limiter puts a stringent requirement on the VSWR of the antenna used with this circulator duplexer. A large reflection from the antenna would consequently nullify the duplexing action of the circulator. A ferroelectric limiter was designed to handle somewhat greater powers in order to protect the limiter rated at 10 kw peak power. This ferroelectric device is presently being evaluated for use in the circulator system.

The circulator enclosure, electro-magnet, power supply, cooling unit and limiter are mounted in a standard 19" relay cabinet which measures 47-1/2" high by 22" deep. The controls necessary for the adjustment of circulator performance are mounted on the front panel.

High power tests were performed at the Naval Research Laboratory (Chesapeake Bay Annex) on the prototype Y-circulator. The power level of the transmitter was gradually increased to its maximum output. At .466 mw there was a high voltage arc-over in the coaxial transition at the input to the circulator. This malfunction was due to a sharp edge on the center conductor of the transition. The faulty component was returned to the company for modification, which consisted mainly in having the sharp edge simply "rounded off". As a further precaution to any further breakdown in this region, the transition was filled with a high dielectric strength gas such as Sulfur-Hexafluoride (SF_6). After this modification the circulator tests were continued with satisfactory results.

2.2 Measurement Procedures

Figures 1, 2, 3, and 4 depict the instrumentation used in performing high voltage, isolation vs temperature at low RF input, dielectric constant vs temperature, and limiter recovery time measurements, respectively. The setup for the measurement of the performance of the complete prototype circulator is shown in Figure 5.

2.3 References

- (1) "Final Development Report for Low Frequency Broad-band Ferrite Components," 30 June 1961; Contract No. NObsr-77602, Index No. NE050500/S. T. 17.4
- (2) "UHF Ferroelectric Phase Shifter Research," Final Report, 30 April 1962; Contract No. AF 19(604)-8379

2.4 Definition of Symbols

mw - megawatt
RF - radio frequency
kw - kilowatt
dc - direct current
db - decibel
BTUH - British thermal unit hours
GPM - gallons per minute

2.5 Identification of Technical Personnel

		<u>Hours</u>
J. C. Wiltse	Manager Microwaves	19
Marvin Cohn	Research Scientist	102
A. F. Eikenberg	Senior Engineer	1548
P. W. Richardson	Senior Draftsman	2
R. Hanna	Senior Draftsman	78
W. C. Yaeger	Draftsman	56
J. D. Rodgers	Junior Engineer	29
G. J. Junggust	Junior Engineer	68

2.6 Patents

None

3. DETAIL FACTUAL DATA

3.1 Circulator Components

A new ferrite disc enclosure was constructed for the prototype Y-circulator. This fabrication was necessary because of the reduced size of the pipe fittings used with the new cooling system. The transmitter and antenna ports are fed by "3-1/8" to type "N" adapters manufactured by Andrew Corporation (Model #2262). The receiver port is fitted with a type "HN" - UG 560 receptacle. Freon 113 dielectric fluid is used as the cooling agent which flows through the ferrite enclosure. This fluid also fills that part of the 3-1/8" adapters which reduces to type "N" dimensions, enabling one to apply large signal strengths without voltage breakdown. The cooling fluid lines and the 3-1/8" to type "N" transitions can be seen in Figure 6 which is a top view photograph of the circulator.

The electromagnet used in the prototype model is the same one that was used in the experimental model. A field of 1000 oersteds in an air gap of 1.625 inches can be obtained with this magnet.

A current regulated dc power supply provides the current for the coils of the electromagnet. The output voltage is of the order of 10 vdc across the magnet coil which has a resistance of 7.5 ohms. A ten turn helipot controls the current output of the power supply, which is continuously adjustable from 0 to 1.65 amperes.

Cooling for the circulator element is provided by a combination refrigeration-pump package manufactured by Budd Electronics.* This unit is capable of delivering 4.4 GPM of Freon 113 at 40 psig to the ferrite enclosure. The maximum cooling capacity is 1880 BTUH which is enough to handle a heat load of 550 watts in the circulator. At 2000 watts of cw power the heat dissipation in the ferrite enclosure is only 200 watts. Considerably more cw power could be applied to the circulator than has been tried, and the cooling system would handle it.

* A division of Budd Company, Inc., Long Island City, New York

The limiter supplied with the circulator package was obtained from Micro-State Electronics. Figure 7 shows the characteristics of this device. Low insertion loss and greater than 40 db of limiting with a 10 nanosecond recovery time makes this unit suitable for use with the circulator. The maximum peak power which can be applied to this limiter is 10 kw. This power rating puts a restriction on the VSWR of the antenna used with the circulator. Assuming a 1 mw input to the circulator the antenna VSWR would have to be < 1.23 in order to prevent limiter burnout. Unfortunately the VSWR of the antenna to be used with the circulator ranges from 1.7 to 2.0. This corresponds to a 7 to 11 percent reflection of input power respectively. With a 1 mw input the reflected power would be 70 kw to 110 kw. Clearly then the limiter presently used in the circulator package is inadequate for the power input and VSWR values mentioned. One could reduce the input power; get an antenna with a lower VSWR; or obtain a limiter with higher power handling capacity. An effort is now being made by this company to develop such a limiter.

3.2 Ferroelectric Limiter

A general need exists for fast acting, high power limiters. Within this contract program, a specific need exists for a high power pre-limiter to precede the previously mentioned semiconductor limiter. A program, partially supported by ECI funds, was initiated to determine the feasibility of a ferroelectric limiter. Since the nonlinear action of such a device takes place within a bulk ceramic material, a high power handling capability was expected. A deterrent to the use of ferroelectric materials in devices such as high power limiters is the lack of sufficient data on the electrical properties of these materials. This is particularly true in the case of their large signal properties; knowledge of which is essential in order to design and predict the performance of limiters.

3.3 Properties of the Ferroelectric Materials

The ferroelectric material used was a ceramic mixture of 45% lead titanate and 55% strontium titanate. This mixture is referred to in mole percent. Its small signal electrical properties were determined from measurements made on small circular parallel plate capacitors fabricated from the same bar of material as was used to fabricate the pellets used in the limiter. The small ferroelectric capacitor (diameter = .033", height = .050") was located between the end of the center conductor and an end plate of a special coaxial holder. A diagram of the measurement system is shown in Figure 3. The assembly was surrounded by a heating coil. A thermocouple was mounted on the coaxial holder to monitor temperature. DC voltages up to 2000 volts could be applied to the ferroelectric capacitor.

The small signal dielectric constant (K) and dielectric loss tangent of two different specimens of the 45% PbTiO_3 - 55% SrTiO_3 ceramic material were measured as a function of temperature (T) and applied dc electric field (E_{dc}) at a frequency of 218 Mc. The two specimens were fired at different temperatures. These small signal properties were determined from standard input impedance measurements made with a slotted line. Curves of the dielectric constant and loss tangent as a function of temperature are shown in Figure 8. The ferroelectric material used in the limiter (UR 5324) has a Curie temperature of 115.75°C . Curves of the dielectric constant and loss tangent of this material as a function of applied dc electric field are presented in Figure 9. The dielectric constant curves are believed to be quite accurate as these readings depend primarily on the location of the VSWR minimum produced by the ferroelectric capacitor. Since the VSWR's were very high, the minimums were located very accurately. The loss tangent curves are considerably less accurate, since the values of loss tangent depend primarily on the magnitude of the VSWR relative to the magnitude of the VSWR produced by a short circuit. The

short circuit consists of a copper cylinder, whose dimensions are the same as those of the ferroelectric capacitors. Since the VSWR's due to the ferroelectric capacitor were only slightly less than that due to the short circuit, a small error in the VSWR measurement could result in a large error in the loss tangent. A few loss tangent measurements (see Section 3.7). were made in a cavity resonator. These measurements, which are far more accurate for low loss materials, indicate that the small signal dielectric loss tangent is substantially lower than indicated in Figures 8 and 9.

Some limited large signal data on the dependence of the dielectric constant on the RF electric field can be deduced from measurements made on the ferroelectric limiter (see Section 3.6). Considerably more data on the large signal properties of ferroelectric materials is sorely needed.

3.4 Construction of the Limiter

The ferroelectric limiter consists of a symmetrical, loop coupled, capacity loaded, coaxial line cavity as shown in Figure 12. A large portion of the capacity loading is provided by the ferroelectric pellet. Due to the large amount of capacitive loading yielded by the very high dielectric constant ferroelectric material, the cavity length is well under a quarter wavelength. An electric heater is located outside of the cavity, but near the ferroelectric pellet in order to bring the pellet temperature within a few degrees of its Curie temperature. The cavity contains a movable short circuit for resonating it at the desired frequency.

The ferroelectric pellet is in the shape of a circular cylinder of radius r_f and height d_f . The remainder of the capacity loading is essentially an air filled parallel plate capacitor of radius r_a and height d_a . Figure 12 contains an expanded drawing of the region near the ferroelectric pellet. The pellet is attached to brass rods set in a well of greater spacing than the remainder of the air

filled capacitor ($> d_a$) in order to increase its resistance to high voltage breakdown. High voltage breakdown is further retarded by coating the lateral surfaces of the ferroelectric pellet and its supporting brass posts with corona dope. These brass posts, whose radii are equal to the pellet radius, are the principle means of removing heat from the ferroelectric pellet. The well surrounding the pellet reduces the air filled capacitor region by only a negligible amount. The entire assembly is filled with sulfur hexafluoride gas (SF_6) at an absolute pressure of one atmosphere.

3.5 Principle of Operation

At low power levels, the limiter structure acts as a low insertion loss transmission cavity tuned to the signal frequency. As the power level increases, the high RF electric fields developed within the cavity cause the dielectric constant of the ferroelectric pellet to change, thus detuning the cavity. The detuned cavity causes most of the incoming power to be reflected at the input port. Similar reflections at the output port result in increased dissipative losses within the cavity.

Starting with the following well known formula for the transmission factor (γ) of a cavity,

$$\gamma(P) = \frac{\gamma_o}{1 + Q_L^2 \left(\frac{f}{f_o} - \frac{f_o}{f} \right)^2} = \frac{\gamma_o}{1 + Q_L^2 \left[\left(\frac{f}{f_o} \right)^2 + \left(\frac{f_o}{f} \right)^2 - 2 \right]} \quad (1)$$

an approximate analysis of the performance of the ferroelectric limiter can be performed. In the above formula, the symbols have the following meaning

$\gamma(P) \leq 1$ is the power transmission factor, which is a function of the RF electric field intensity

$\gamma_o \leq$ is the power transmission factor at low RF power levels

Q_L is the loaded Q of the cavity

f is the signal frequency

f_o is the resonant frequency of the cavity

$$f_o = \frac{1}{4\pi^2 L (C_a + C_f)} = \frac{1}{4\pi^2 L C_a (1 + C_f/C_a)} \quad (2)$$

where L is the inductance due to the length of short circuited coaxial transmission line, and C_a and C_f are respectively the values of capacitive loading due to the air filled and ferroelectric filled end loading. The ferroelectric capacitor is assumed to have the following functional dependence on the RF electric field intensity.

$$C_f = \epsilon_o (K - K_1 E_{RF}) \frac{A_f}{d_f} \quad (3)$$

$$C_a = \epsilon_o \frac{A_a}{d_a} \quad (4)$$

A_f , d_f , A_a and d_a are the areas and heights of the ferroelectric filled and air filled parallel plate capacitor regions. In this approximate analysis, fringe fields are neglected. From equations (2), (3) and (4),

$$f_o^2 = \frac{1}{4\pi^2 L C_a \left[1 + (K - K_1 E_{RF}) \left(\frac{A_f}{A_a} \right) \left(\frac{d_a}{d_f} \right) \right]} \quad (5)$$

The signal frequency, which equals the resonant frequency at low power levels, is given by

$$f_o^2 = f_o^2 (E_{RF} + 0) = \frac{1}{4\pi^2 L C_a \left[1 + K \left(\frac{A_f}{A_a} \right) \left(\frac{d_a}{d_f} \right) \right]} \quad (6)$$

$$\therefore \frac{f}{f_o} = 1 - \frac{K_1 E_{RF} \left(\frac{A_f}{A_a} \right) \left(\frac{d_a}{d_f} \right)}{1 + K \left(\frac{A_f}{A_a} \right) \left(\frac{d_a}{d_f} \right)}, \text{ and} \quad (7)$$

$$\left(\frac{f_o}{f}\right)^2 = \frac{1}{1 - \frac{K_1 E_{RF} \left(\frac{A_f}{A_a}\right) \left(\frac{d_a}{d_f}\right)}{1 + K \left(\frac{A_f}{A_a}\right) \left(\frac{d_a}{d_f}\right)}} \quad (8)$$

Equation 8 can be rewritten in the following form

$$\left(\frac{f_o}{f}\right)^2 = 1 + \sum_{k=1}^{\infty} \left[\frac{K_1 E_{RF} \left(\frac{A_f}{A_a}\right) \left(\frac{d_a}{d_f}\right)}{1 + K \left(\frac{A_f}{A_a}\right) \left(\frac{d_a}{d_f}\right)} \right]^k \quad (9)$$

$$\therefore \gamma(P) = \frac{\gamma_o}{1 + Q_L^2 \sum_{k=2}^{\infty} \left[\frac{K_1 E_{RF} \left(\frac{A_f}{A_a}\right) \left(\frac{d_a}{d_f}\right)}{1 + K \left(\frac{A_f}{A_a}\right) \left(\frac{d_a}{d_f}\right)} \right]^k} \quad (10)$$

The RF electric field appearing across the ferroelectric capacitor is related to the available input power from the generator (P_{in}) by the following equation:

$$E_{RF} = \frac{n}{d_f} \sqrt{4 P_{in} Z_o} \quad (11)$$

where Z_o is the characteristic impedance of the input and output transmission lines and n is the equivalent transformer turns ratio of the input and output coupling loops. The equivalent turns ratio (n) is related to the cavity coupling coefficient (β) and the equivalent shunt resistance of the unloaded cavity (R_f) by the following equation.

$$n = \sqrt{\frac{R_f}{B Z_o}} \quad (12)$$

This shunt resistance is assumed to be totally due to dielectric losses within the ferroelectric pellet.

$$\therefore R_f = \frac{1}{2\pi f C_f \tan \delta} \quad (13)$$

In this approximate analysis, both β and R_f are assumed to be independent of E_{RF} . The low power transmission factor γ_o is related to the coupling coefficient by the following well known relationship

$$\gamma_o = \frac{4\beta^2}{(1 + 2\beta)^2} \quad (14)$$

$$\gamma(P) = \frac{\gamma_o}{1 + Q_L^2 \sum_{k=2}^{\infty} \left[\frac{K_1 \left(\frac{A_f}{A_a}\right) \left(\frac{d_a}{d_f}\right) \frac{2n}{d_f}}{1 + K \left(\frac{A_f}{A_a}\right) \left(\frac{d_a}{d_f}\right)} (Z_o)^{1/2} (P_{in})^{1/2} \right]^k} \quad (15)$$

For $\frac{K_1 \left(\frac{A_f}{A_a}\right) \left(\frac{d_a}{d_f}\right) \frac{2n(Z_o)^{1/2}}{d_f}}{1 + K \left(\frac{A_f}{A_a}\right) \left(\frac{d_a}{d_f}\right)} (P_{in})^{1/2} \ll 1,$

which is the case for the ferroelectric material used ($K_1 \ll K$) and the input power levels studied, only the first term of the series need be retained

$$\therefore \gamma(P) = \frac{\gamma_o}{1 + Q_L^2 \left[\frac{K_1 \left(\frac{A_f}{A_a}\right) \left(\frac{d_a}{d_f}\right) \frac{2n}{d_f}}{1 + K \left(\frac{A_f}{A_a}\right) \left(\frac{d_a}{d_f}\right)} Z_o P_{in} \right]^2} \quad (16)$$

$$\text{Let } P_c = \left\{ Q_L^2 \left[\frac{K_1 \left(\frac{A_f}{A_a} \right) \left(\frac{d_a}{d_f} \right) \frac{2n}{d_f}}{1 + K \left(\frac{A_f}{A_a} \right) \left(\frac{d_a}{d_f} \right)} \right]^2 Z_o \right\}^{-1} \quad (17)$$

$$\therefore P_{out} = \gamma(P) P_{in} = \frac{\gamma_o P_{in}}{1 + \frac{P_{in}}{P_c}} \quad (18)$$

For $P_{in} \ll P_c$, Equation 18 reduces to the usual linear function.

$$P_{out} = \gamma_o P_{in} \quad (P_{in} \ll P_c) \quad (19)$$

For $P_{out} \ll P_c$, Equation 18 shows that the output power reaches a constant saturation level.

$$(P_{out})_{sat} = \gamma_o P_c \quad (P_{in} \gg P_c) \quad (20)$$

For $P_{in} = P_c$, which could be called a corner power level,

$$P_{out} = \frac{\gamma_o P_c}{2} = \frac{(P_{out})_{sat}}{2} \quad (P_{in} = P_c) \quad (21)$$

Some measured P_{out} versus P_{in} curves for this type of limiter are presented in Section 3.7. The shape of these curves illustrate the type of behavior predicted by Equation 18. Equations 17 and 18 indicate how the performance of these limiters can be adjusted through control of the geometry (A_f , A_a , d_f , d_a) and the coupling coefficient and loaded Q of the cavity (β , n , Q_L).

From measurements of $(P_{out})_{sat}$, one can determine the value of K_1 and hence the large signal value of the dielectric constant as a function of E_{RF} . Measurements on two limiters have yielded the following values of large signal dielectric constant:

$$\epsilon(E_{RF}) = \epsilon_0 (4806 - 1.96 \times 10^{-4} E_{RF}) \text{ and}$$

$$\epsilon(E_{RF}) = \epsilon_0 (4806 - 3.82 \times 10^{-4} E_{RF}),$$

Where E_{RF} is given in volts per meter. The difference between the two values of K_1 measured on two different pellets of nominally the same material may be due in part to different operating temperatures of the pellets. The temperature rise of the pellets due to RF power dissipation is discussed in Section 3.6.

Some previous large signal measurements^{3,4} made on a different ceramic ferroelectric material at higher frequencies have indicated that the dependence of the dielectric constant on E_{RF} is of the form, $\epsilon = \epsilon_0 (a - b E_{RF}^2)$. The above quadratic functional dependence on E_{RF} , however, results in a calculated power out versus power in characteristic which reaches a maximum value and then decreases again. An excellent fit with experimental data was obtained through the assumed use of a dielectric constant which varies linearly with E_{RF} .

3.6 Temperature Rise and Thermal Relaxation

It is well known that the change of the dielectric constant of ferroelectric materials as a function of dc electric field intensity is dependent on temperature. Although very little data is available on the large signal properties of ferroelectric materials, it is likely that the change of dielectric constant as a function of the RF electric field intensity is similarly temperature dependent. In order to obtain

3. D.A. Johnson, "Microwave Properties of Ceramic Nonlinear Dielectrics," Microwave Lab. Rpt. No. 825, Stanford University, Contract No. AF 49(638)-514; July, 1961.
4. M. DiDomenico, D.A. Johnson, and R.H. Pantell, "A Ferroelectric Harmonic Generator and the Large Signal Microwave Characteristics of a Ferroelectric Ceramic," Internal Memorandum M. L. No. 862, Stanford University, October, 1961.

proper operation of the limiter, it is essential that the ferroelectric pellet be maintained within the proper temperature interval (close to the Curie temperature) despite the fact that RF power is dissipated in the pellet. An excessive temperature within the pellet will cause the limiter cavity to be detuned. It is essential to the operation of the limiter that the detuning be due to high electric field intensity rather than a temperature change for the following reasons.

- (1) To obtain rapid response in order to avoid spike leakage
- (2) To achieve rapid recovery, so that a low level signal following shortly after the high power pulse is not attenuated.

In order to estimate both the expected temperature rise due to RF dissipation and the thermal response time of the limiter, an idealized analysis was performed. The specific heat (C_p) and density (ρ) of two different batches of the ferroelectric material were measured and used in this analysis. The pertinent properties of these two materials are shown in Table I.

<u>Ferroelectric Material</u>	<u>UR 5324</u>	<u>UR 5359</u>
Constituents	45% PbTiO ₃ 55% SrTiO ₃	45% PbTiO ₃ 55% SrTiO ₃
Firing Temperature	1272°C	1230°C
Curie Temperature (T_c)	115.75°C	118°C
Specific Heat (C_p)	0.15 ± .02	0.11 ± .02
Density (ρ) (grams/cm ³)	5.54 ± .01	5.53 ± .01

TABLE I

The analysis of the thermal system assumes that initially the ferroelectric pellet is at the same temperature (T) as the cavity. The only source for differential heating of the pellet is the RF power dissipated P_d within it. Heat can be transferred from the ferroelectric pellet to the

remainder of the cavity only via conduction through the metal posts which contact the circular faces of the pellet. The pertinent parameters of the posts are their thermal conductivity (k), cross-sectional area ($A = \pi r_f^2$), and their length (S).

The heat energies introduced (q_{in}) and extracted (q_{out}) from the ferroelectric pellet are

$$q_{in} = P_d t \quad (22)$$

and

$$q_{out} = \frac{kA}{s} \Delta T t, \quad (23)$$

where ΔT is the temperature rise of the pellet and t is the time measured from the instant when the RF power is applied. The incremental energy stored in the pellet (q_{stored}) is

$$q_{stored} = m C_p \Delta T, \quad (24)$$

where m and C_p are the mass and specific heat of the pellet. The heat balance equation requires that

$$q_{in} - q_{out} = q_{stored} \quad (25)$$

Substituting Equations 22, 23, and 24 into 25 one obtains the following equation for the temperature rise of the pellet as a function of time.

$$\Delta t = \frac{P_d t}{m C_p + \frac{kA}{s} t} \quad (26)$$

The equilibrium temperature rise is given by the following equation.

$$\lim_{t \rightarrow \infty} \Delta T = \frac{S P_d}{kA} \quad (27)$$

Let

$$\Delta T(t) = r \frac{S P_d}{kA} \quad (28)$$

where $0 \leq r \leq 1$, and is the ratio of the instantaneous temperature rise to the final equilibrium temperature rise. From Equation 26 and 28, an expression for the time required for the ferroelectric pellet to reach any fraction of its final equilibrium temperature rise is obtained.

$$t_r = \frac{S m C_p}{kA} \cdot \frac{r}{1-r} \quad (29)$$

The time required to reach half of its final value ($r = 0.5$) is

$$t_{0.5} = \frac{S m C_p}{kA} \quad (30)$$

Using the proper material constants and geometric parameters the half time ($t_{0.5}$) for a limiter containing a pellet of UR 5324 can be calculated. The values used are those which apply to a limiter whose performance is discussed in Section 3.7 ($r_f = .0165''$, $d_f = .080''$).

$$S = .035'' = .089 \text{ cm}$$

$$A = 2A_f \text{ (two posts)} = 2\pi(r_f)^2 = 1.102 \times 10^{-2} \text{ cm}^2$$

$$k = .26 \text{ calories/cm-sec-}^\circ\text{C (brass)}$$

$$C_p = .15 \text{ calories/gram-}^\circ\text{C}$$

$$\rho = 5.54 \text{ gm/cm}^3$$

$$\therefore m = \rho A_f d_f = 6.2 \times 10^{-3} \text{ grams.}$$

$$\therefore t_{0.5} = 28.9 \text{ milliseconds}$$

The above measure of the response time is very long compared to typical pulse lengths (T_p) of high power systems. For $t \approx T_p \ll t_{0.5}$, Equation 26 can be approximated as follows.

$$\Delta T = \frac{P_d}{m C_p} t \quad (31)$$

Thus at the end of the first pulse ($t = T_p$), the pellet temperature will have risen an amount a given by

$$a = \frac{P_d T_p}{m C_p} \quad (32)$$

At the cessation of the pulse, the pellet temperature decreases according to the following relationship.

$$\Delta T = \frac{a}{1 + t/t_{0.5}} \quad (33)$$

During the time interval between pulses (θ), ΔT will decrease but not reach zero. It will decrease to a value given by

$$\Delta T = \beta = \frac{a}{1 + \theta/t_{0.5}} \quad (\text{at } t = T_p + \theta) \quad (34)$$

After successive intervals of T and θ , the temperature difference will follow a sequence as listed below.

t	ΔT
0	0
t	a
$t + \theta$	$a \left[\frac{1}{1 + (\theta/t_{0.5})} \right]$
$2t + \theta$	$a + a \left[\frac{1}{1 + (\theta/t_{0.5})} \right]$
$2t + 2\theta$	$a \left[\frac{1}{1 + (\theta/t_{0.5})} \right] + a \left[\frac{1}{1 + (\theta/t_{0.5})} \right]^2$
$nt + (n-1)\theta$	$a \sum_{k=0}^{n-1} \left[\frac{1}{1 + (\theta/t_{0.5})} \right]^k$
$nt + n\theta$	$a \sum_{k=1}^n \left[\frac{1}{1 + (\theta/t_{0.5})} \right]^k$

TABLE II

After steady state has been reached ($n \rightarrow \infty$), the pellet temperature will vary between the limits determined by the sum of the geometric series listed in Table II. At $t = nt + (n-1)\theta$:

$$\Delta T = (\Delta T)_{\max} = \frac{a}{1 - \frac{1}{1 + (\theta/t_{0.5})}} = a \left[\frac{t_{0.5}}{\theta} \right] + 1 \quad (35)$$

At $t = nt + n\theta$

$$\Delta T = (\Delta T)_{\min} = a \left[\frac{t_{0.5}}{\theta} \right] + 1 \left[\frac{1}{1 + (\theta/t_{0.5})} \right] = a \frac{t_{0.5}}{\theta} \quad (36)$$

Substituting Equations 30 and 32 into 35 and 36, one obtains the following values for the limits of the temperature excursion after steady state conditions have been reached.

$$(\Delta T)_{\min} = \frac{P_d T_p S}{kA\theta} \quad (37)$$

$$(\Delta T)_{\max} = \frac{P_d T_p S}{kA\theta} + \frac{P_d T_p}{m C_p} \quad (38)$$

In the case of the previously discussed limiter configuration (see Section 3.4), having a response time of 28.9 milliseconds, it was found that a peak power input of 26.3 kw resulted in a reflected and transmitted power levels of 23.4 kw and 0.22 kw respectively. The peak power dissipated (P_d) was thus 2.68 kw (640 calories/sec). It will be assumed that all of this power was dissipated within the ferroelectric pellet. In this case $T_p = 8 \times 10^{-6}$ seconds, and $\theta = 16.67 \times 10^{-3}$ seconds (60 pulses per second). Using Equations 37 and 38, it is found that

$$(\Delta T)_{\min} = 9.55^\circ \text{C}$$

and

$$(\Delta T)_{\max} = 15.05^\circ \text{C} .$$

In order that the ferroelectric pellet be at a temperature near its Curie temperature (T_c) after steady state conditions have been reached, the ambient temperature of the cavity should be maintained at a temperature near

$$T = T_c - (\Delta T)_{\max}$$

Spike leakage will be minimized, if the temperature rise during the pulse $[(\Delta T)_{\max} - (\Delta T)_{\min}]$ is minimized. Equation 38 shows that this can be accomplished through the use of a heavier ferroelectric pellet. The above example indicates that recovery time is not a problem, since the pellet temperature will change very little during an interval of a few milliseconds following cessation of the high power pulse.

3.7 Measured Limiter Performance

An attempt was made to develop a traveling wave ferroelectric limiter of the type shown in Figure 10. This surface wave structure had previously been successfully used as a ferroelectric phase shifter.^{5, 6} Such a structure offers the advantage of very high power handling capability. In addition, because of the large ferroelectric slab mass and the large area in intimate contact with the conducting planes, a minimum temperature rise due to RF power dissipation would be expected. Due to (1) the low impedance of this traveling wave structure and (2) the observed fact that $\Delta K/\Delta E_{RF}$ is much less than $\Delta K/\Delta E_{dc}$, insufficient phase shift was developed as a function of the incident RF power level. It may be desirable to re-examine the traveling wave structure for higher power systems.

-
5. M. Cohn and A. F. Eikenberg, "UHF Ferroelectric Phase Shifter Research," Research Div., Electronic Communications, Inc., Timonium, Md., Final Report on Contract No. AF 19(604)-8379; 30 April, 1962.
 6. M. Cohn and A. F. Eikenberg, "Ferroelectric Phase Shifters for VHF and UHF," IRE Trans., Vol. MTT-10, pp. 536-548; November, 1962.

As a result of the above, all efforts on the traveling wave structure were abandoned in favor of the cavity type limiter which was analyzed in Section 3.5. Small signal measurements were made on the cavity type limiter shown in Figure 12. Initially the ferroelectric pellet dimensions were: $r_f = .0165''$, $d_f = .050''$. Typical small signal frequency response curves are shown in Figure 11. Each of these curves is for a different coupling loop size and hence a different coupling coefficient (β). These measurements provided information on the coupling loop configurations needed to obtain desired values of small signal insertion loss (γ_o) and loaded Q (Q_L). Similar measurements were made at various temperatures, and they showed that a low insertion loss can be maintained over a temperature range of a few degrees in the vicinity of the Curie temperature (T_c).

Using the measured values of γ_o and Q_L , β and the unloaded Q (Q_u) can be calculated. The value of Q_u in conjunction with C_a/C_f , as determined from the geometry and small signal dielectric constant measurement, allows one to compute the loss tangent ($\tan \delta$) of the ferroelectric material. The value of $\tan \delta$ as determined from a number of cavity measurements at the Curie temperature is .0037.

High power measurements made on limiters containing these small ferroelectric pellets, indicated that the desired limiting action could be obtained, but high voltage breakdown occurred at input power levels of 10 kw or less. When the pellet height (d_f) was increased to .080'', it was found that input power levels up to 26.3 kw could be handled without adverse effects. Small signal measurements on this limiter showed that the insertion loss (γ_o) was 0.85 db and the loaded Q was 47.5. The measured P_{out} versus P_{in} curve of this limiter is shown in Figure 13. The reflected power is also shown. The measured output power at saturation ($P_{out})_{sat}$ is 224 watts. Using this value of ($P_{out})_{sat}$ and Equation 16, K_1 was determined to be 1.96×10^{-4} meters/volt. This value of K_1 was inserted in Equations 17 and 18 to compute the theoretical P_{out} versus P_{in} curve shown on Figure 13.

It should be noted that the theoretical curve was forced to agree with the measured curve at saturation. The two curves have the same form at lower power levels. This agreement appears to confirm the assumed dependence of the dielectric constant on the RF electric field intensity.

In order to reduce the low level insertion loss and increase the power handling capability by decreasing the internal RF electric field, the coupling coefficient was increased. This was accomplished by using two turn loops at both the input and output. The low level insertion loss was thereby decreased to 0.5 db and the loaded Q reduced to 28.3. The measured P_{out} versus P_{in} curve of this final limiter is shown in Figure 14. The measured $(P_{out})_{sat}$ of 300 watts indicates that K_1 was 3.82×10^{-4} meters/volt. The discrepancy between the two values of K_1 may be due to different pellet temperatures. More extensive large signal measurements are needed to determine K_1 as a function of temperature. The measured and theoretical limiter characteristics shown in Figure 14 are in nearly perfect agreement.

Additional measurements were made on the ferroelectric limiter in order to obtain recovery time data. A series of oscilloscope photographs (Figures 16, 17, 18) show the combined high power, low power signals as they emerge from the limiter. Figure 16 clearly shows the low power pulse visible within the trailing edge of the high power pulse. Figures 17 and 18 show two different positions of the low power pulse with respect to the large signal. These last two photographs were included so that the reader could identify the low level signal as that which is shown in Figure 16. The sweep time calibration for these photographs was set at 20 microseconds per division. A display of both pulses superimposed was not possible because of instrumentation; however, one can see from Figure 16 that the low level pulse is still present well within the large pulse. This indicates that the limiter has a recovery time of less than 10 microseconds. The results of these measurements demonstrate the

fact that the limiter operation is indeed dependent upon the electric field component of the large RF signal rather than its heating effect.

3.8 Circulator Performance at Low Power

Since the circulator was modified by way of new transitions and a new ferrite enclosure, measurements were made to check the low signal isolation-insertion loss characteristics. A diagram of the measuring setup is shown in Figure 2. The transmitter-receiver isolation and the transmitter-antenna insertion loss is shown in Figure 15. An isolation of ≥ 50 db and an insertion loss of 0.5 db shows that good circulator performance was maintained after the aforementioned modifications. It should be pointed out that the temperature scale of Figure 15 is a relative temperature and does not reflect the true temperature of the ferrite discs. The method used in heating the circulator for these measurements was such as to supply heat from the outside. The actual heating of the circulator under high power operating conditions will be from the inside.

3.9 Circulator Performance at High Power

The setup for the measurement of the performance of the prototype high power Y-circulator under actual large signal conditions is shown in Figure 5. The transmitter output was monitored by means of a directional coupler at the input to the circulator. A high power dummy load with a VSWR of 1.05 was connected to the antenna port through another directional coupler. This monitored the transmitter signal coming through the circulator's low loss path.

The power coming out of the isolated port could be monitored through the limiter or through a directional coupler. This was accomplished by means of a coaxial switch which could select either output. The directional coupler position was used when first monitoring the power out of the circulator's isolated port. Once it was determined that the isolation was at least twenty db, the coaxial switch could then be turned to the limiter position. This would insure that the limiter was not being overloaded.

A warm-up period of approximately fifteen minutes is required before the circulator is ready for operation at high power. The ferrite must be at a certain temperature to insure optimum performance. This temperature can be read directly off a meter located on the front panel of the cooling unit. For the circulator to provide at least 20 db isolation the temperature should read $90^{\circ}\text{F} (+5^{\circ} - 1^{\circ})$. Should these values be exceeded the magnetic field would have to be readjusted for maximum isolation.

An SPS/17 Radar Transmitter manufactured by the General Electric Company was used as the source of high RF power. Unfortunately, this source could provide only .640 mw of energy at 1920 watts average power. It was hoped to use a source capable of producing 1 mw of peak power; however, the data obtained with this source at 219.5 Mc is as follows:

Peak Input Power	0.640 mw
Average Input Power	1.920 kw
Isolation (Including Limiter)	70.5 db
Insertion Losses	0.6 db

The circulator functioned normally throughout the high power tests. There was no indication of voltage breakdown or rise in temperature. Further tests would have to be performed using a higher power transmitter in order to determine its full power handling capacity.

4. CONCLUSION

The high power Y-circulator has been tested and delivered to the Chesapeake Bay Annex of the Naval Research Laboratory. High power tests were performed and satisfactory results obtained with a peak power of .640 mw. Higher powers were not available for testing the circulator to its design limit of 1 mw peak power.

Although the circulator is designed for 1 mw, a lower input power might have to be used depending on the VSWR of the antenna employed in the system. A reflection of 10 kw or more will overload the limiter presently supplied in the circulator package.

A ferroelectric limiter has been designed which will handle 20 kw of peak power with approximately 18 db of limiting. Measured performance and a theoretical analysis have shown that excellent limiting characteristics can be obtained through the use of ferroelectric materials. The analysis indicates that saturation power output levels ranging from a few watts on up can be obtained with ferroelectric pellets that can be conveniently fabricated. Additional data on the large signal properties of ferroelectric materials is needed. The limited available material data indicates that ferroelectric limiters will offer their greatest advantage in the HF, VHF, and UHF bands. The theoretical analysis of the expected temperature rise within the ferroelectric pellet has shown that by proper design, very high average power levels can also be handled.

Recommendations

Although the prototype high power Y-circulator has been successfully completed and tested, it is recommended that this unit be made more versatile in its ability to be used with antennas or other loads having a VSWR as high as 2.0. It is imperative in systems using a circulator as a duplexer that the reflected signal be eliminated or attenuated such that it will not damage the front end of a receiver. A high power limiter is one solution to this problem; however, the present "state of the art" limiters have a peak power rating of only

10 kw. In light of the results obtained with the ferroelectric limiter as part of this contract it is entirely feasible that a device capable of 100 kw peak power input can be made.

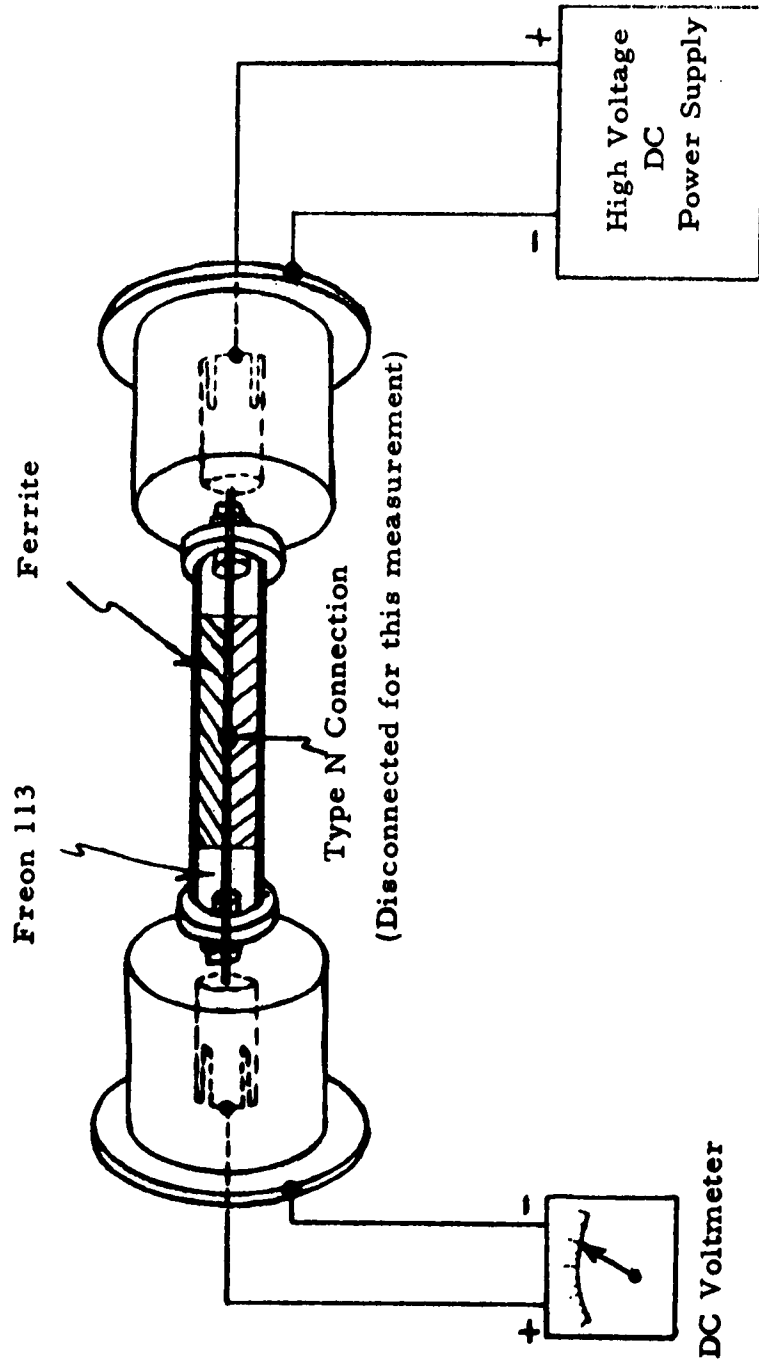
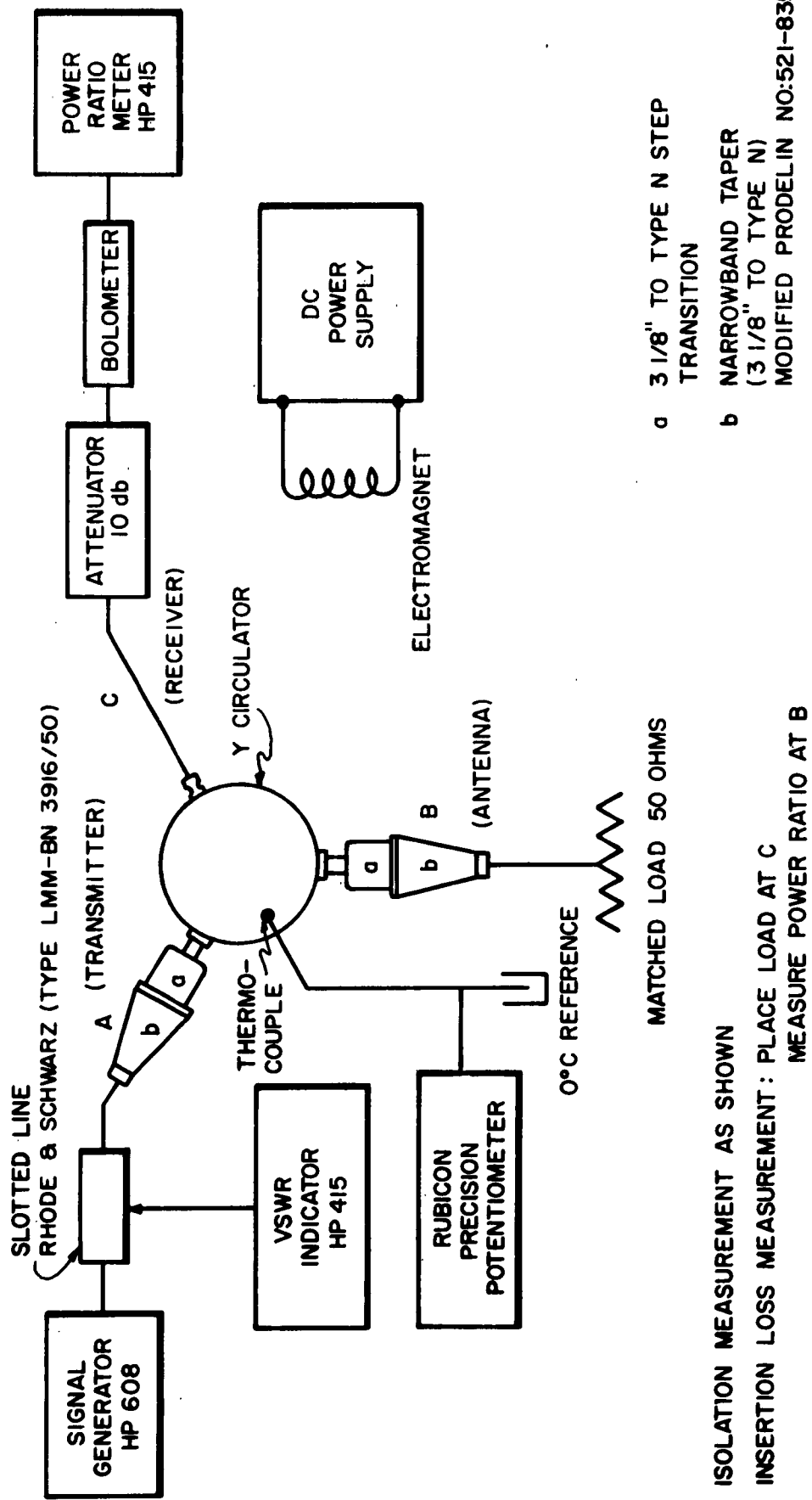


FIGURE 1 - HIGH VOLTAGE TEST



- a 3 1/8" TO TYPE N STEP TRANSITION
- b NARROWBAND TAPER (3 1/8" TO TYPE N) MODIFIED PRODELIN NO:521-835

ISOLATION MEASUREMENT AS SHOWN
 INSERTION LOSS MEASUREMENT: PLACE LOAD AT C
 MEASURE POWER RATIO AT B

FIG. 2 - LOW POWER MEASUREMENT OF HIGH POWER CIRCULATOR

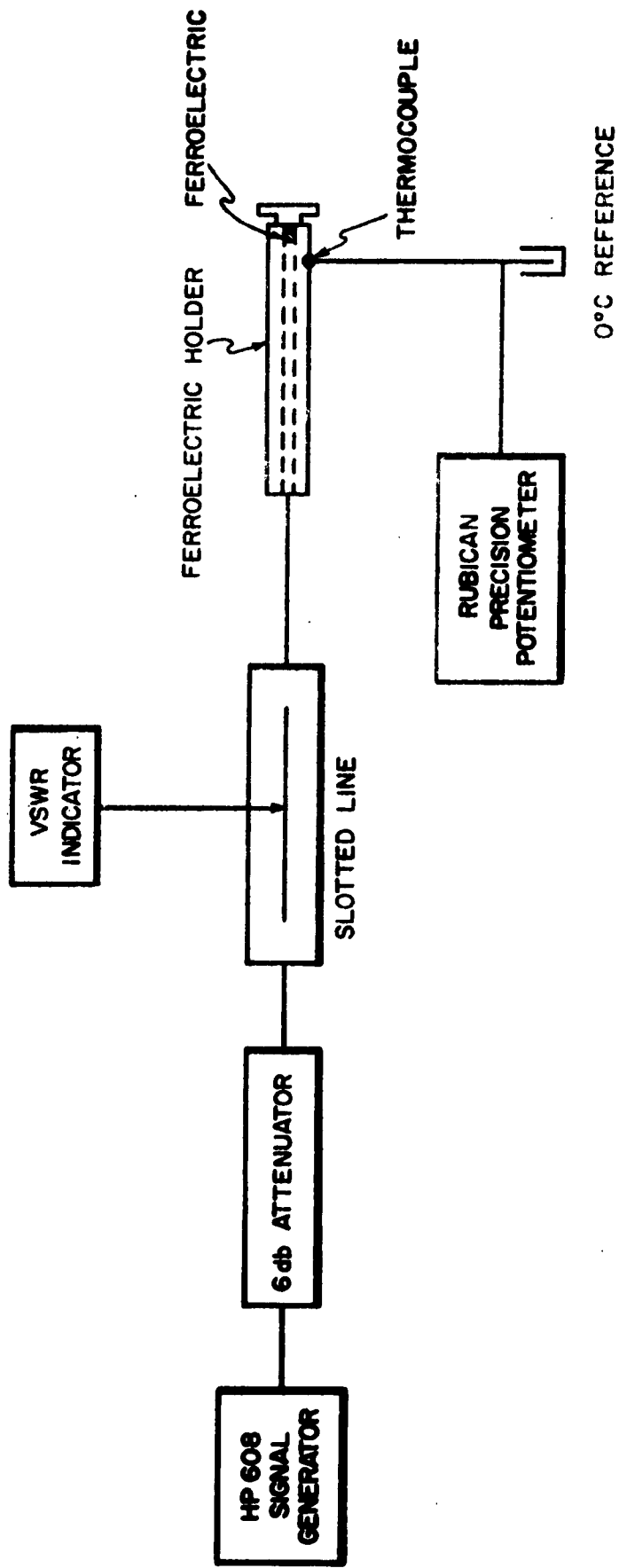


FIG. 3 - MEASUREMENT OF FERROELECTRIC PROPERTIES

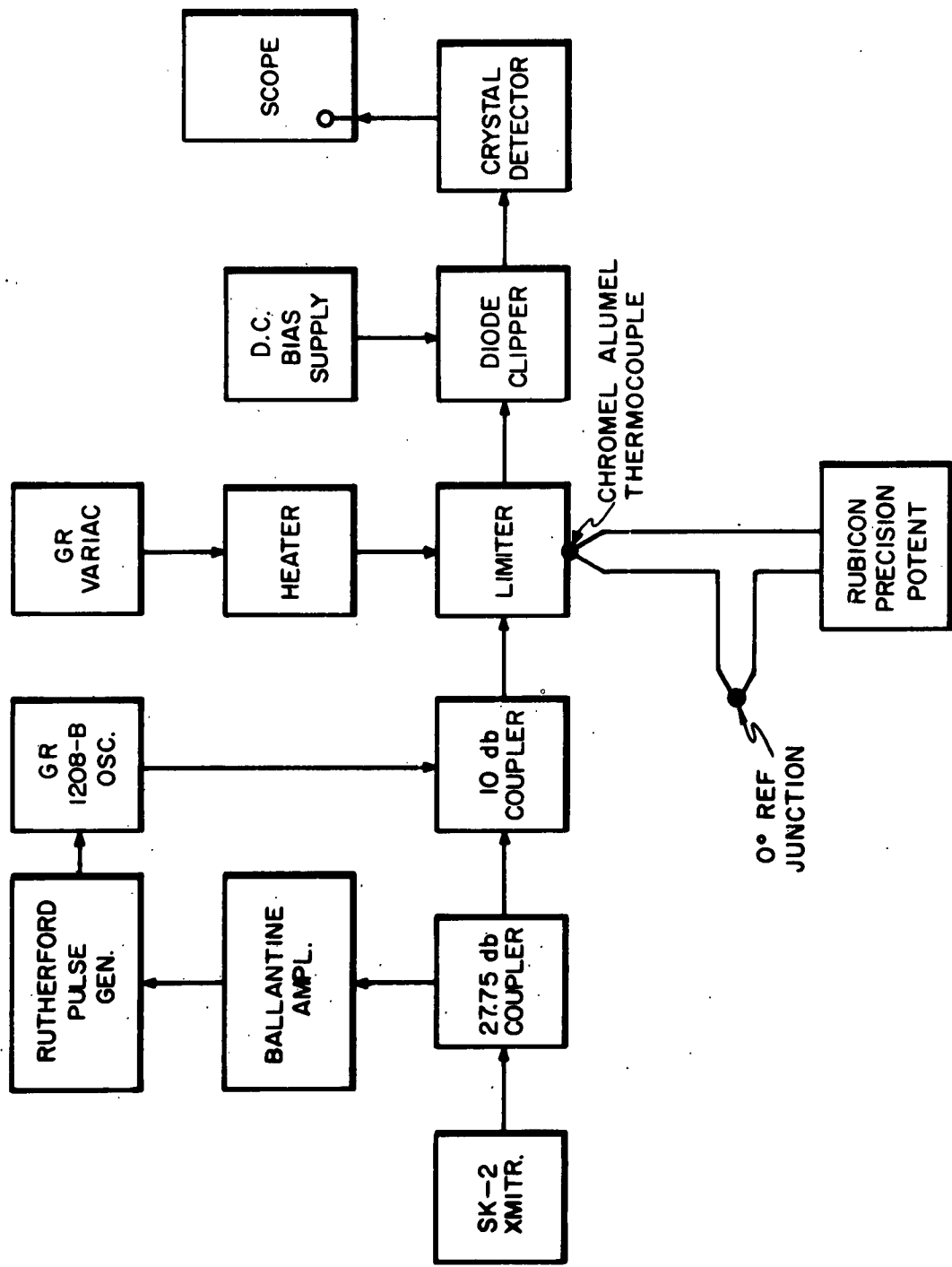


FIG. 4 - SET UP FOR MEASUREMENT OF RECOVERY TIME

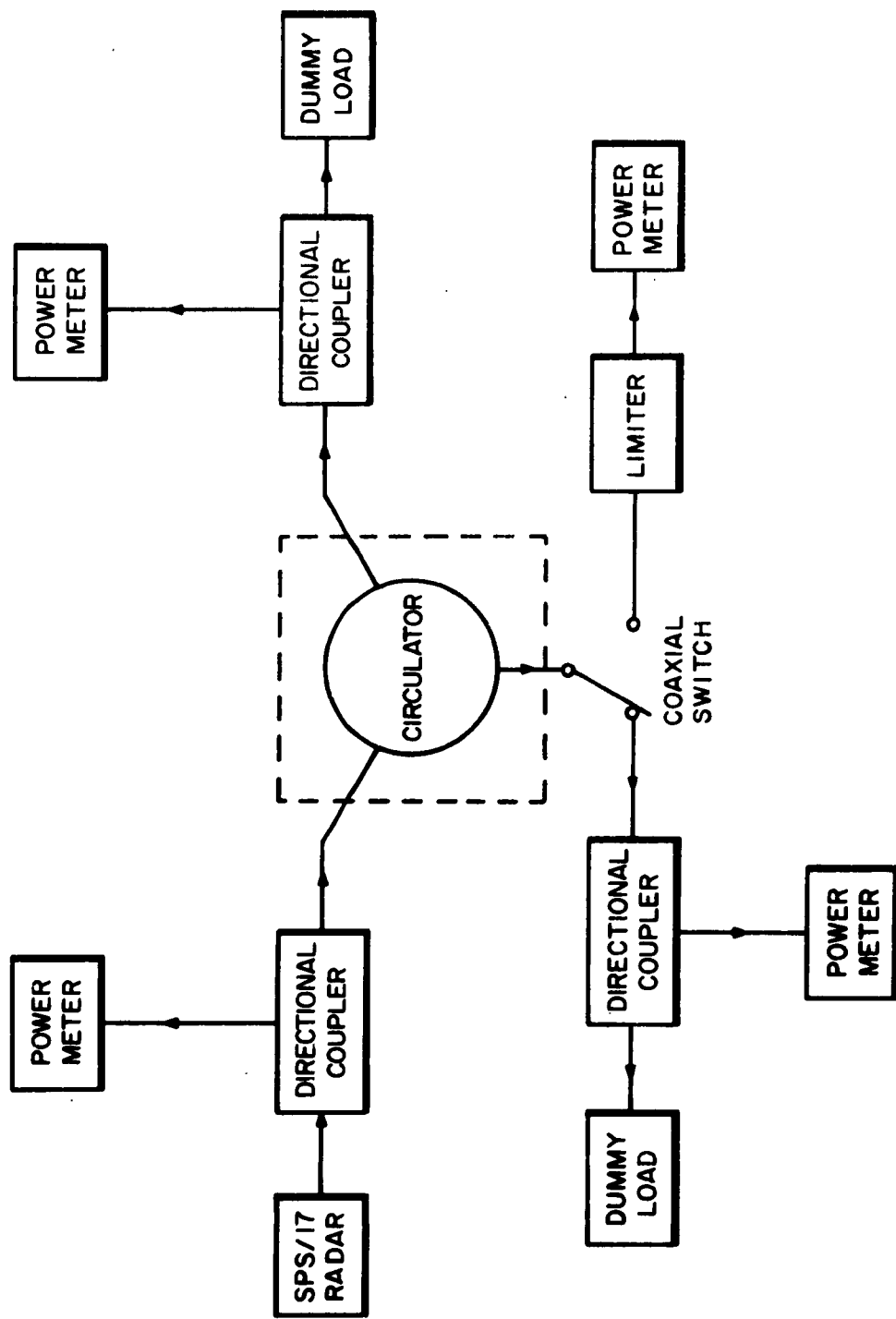


FIG. 5 - HIGH POWER MEASUREMENT SETUP

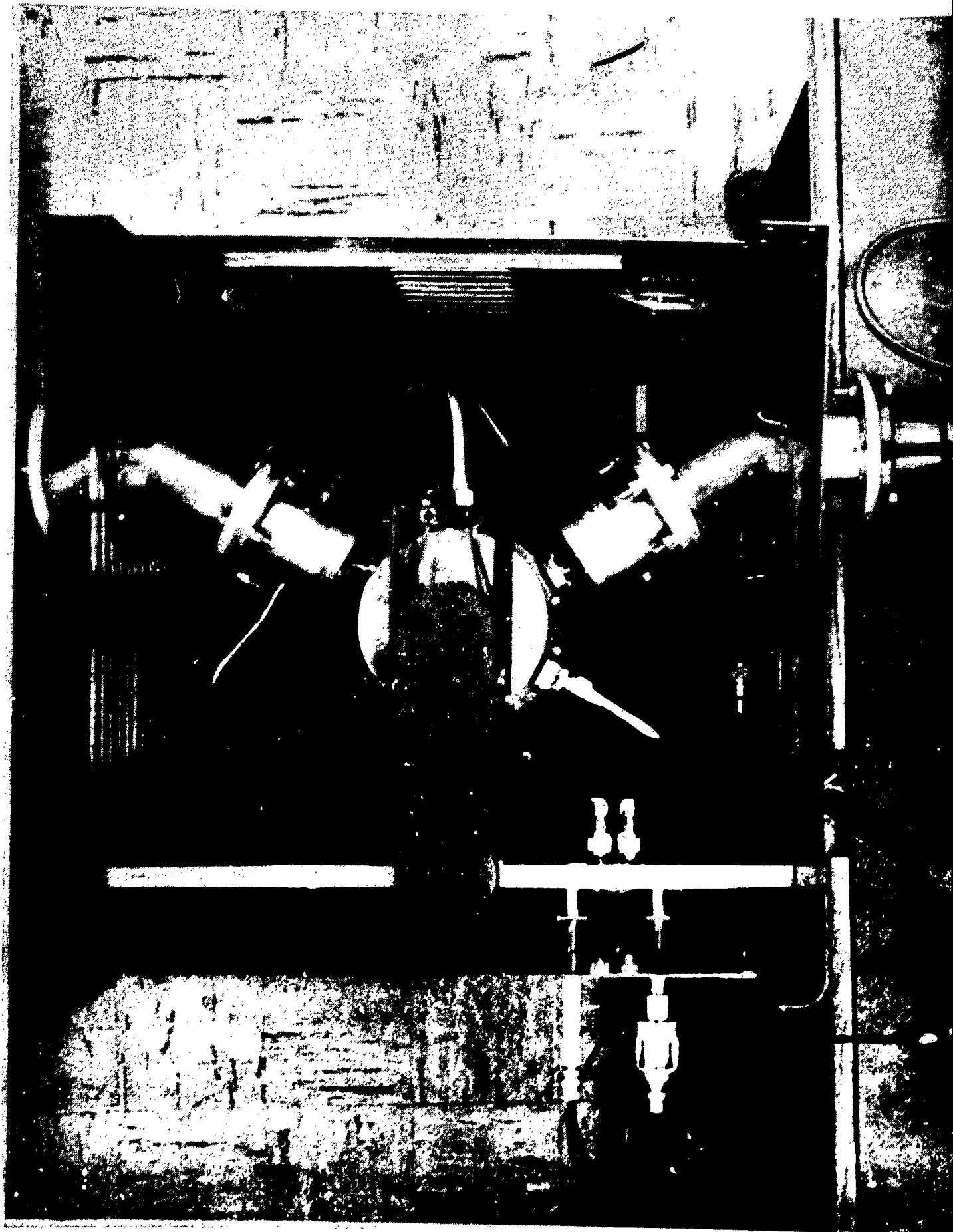


FIG. 6 - TOP VIEW OF HIGH POWER Y-CIRCULATOR

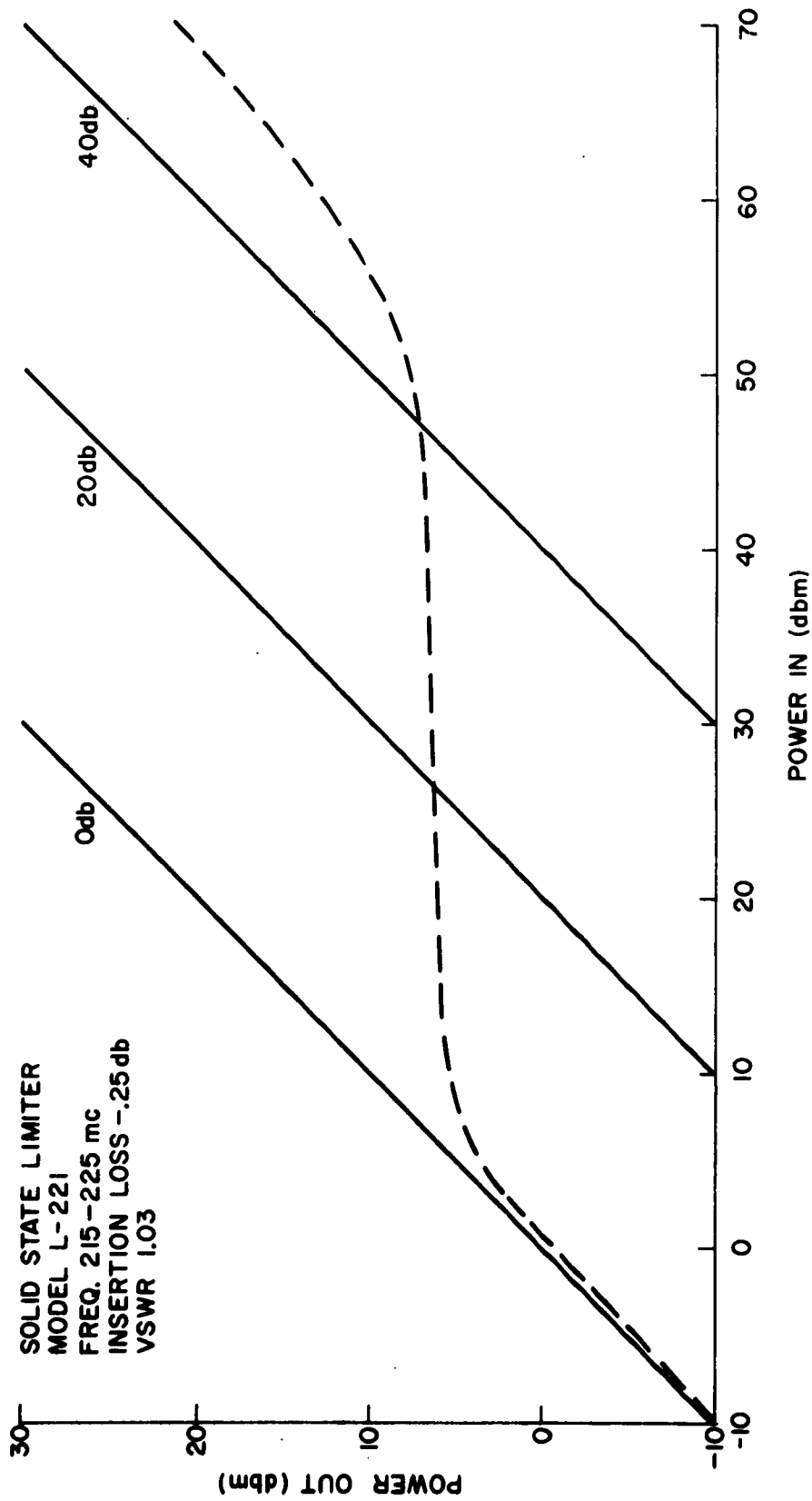


FIG. 7 - CHARACTERISTICS OF MICRO-STATE LIMITER

FIG. 8 - LOSS TANGENT AND DIELECTRIC CONSTANT vs TEMPERATURE

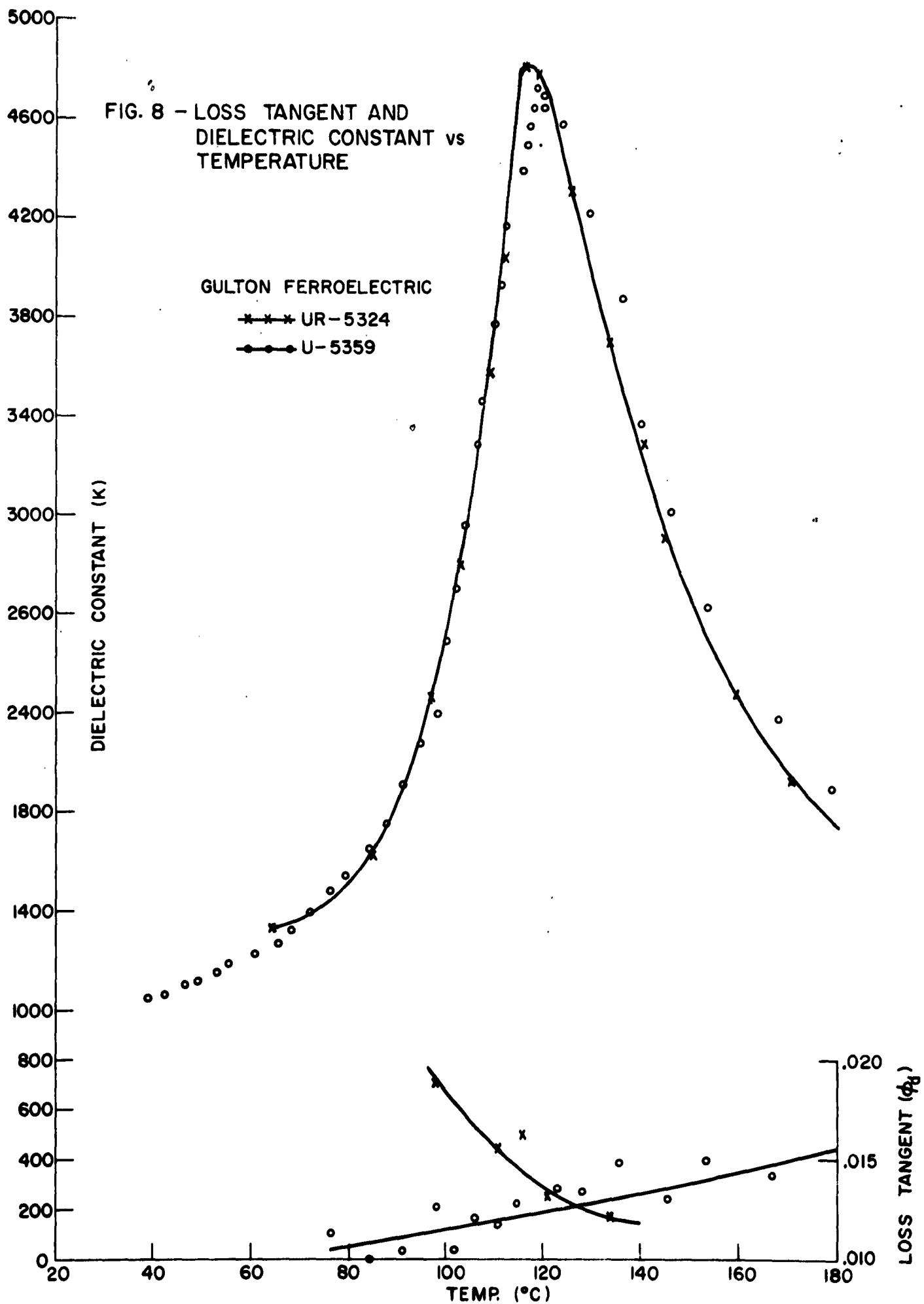
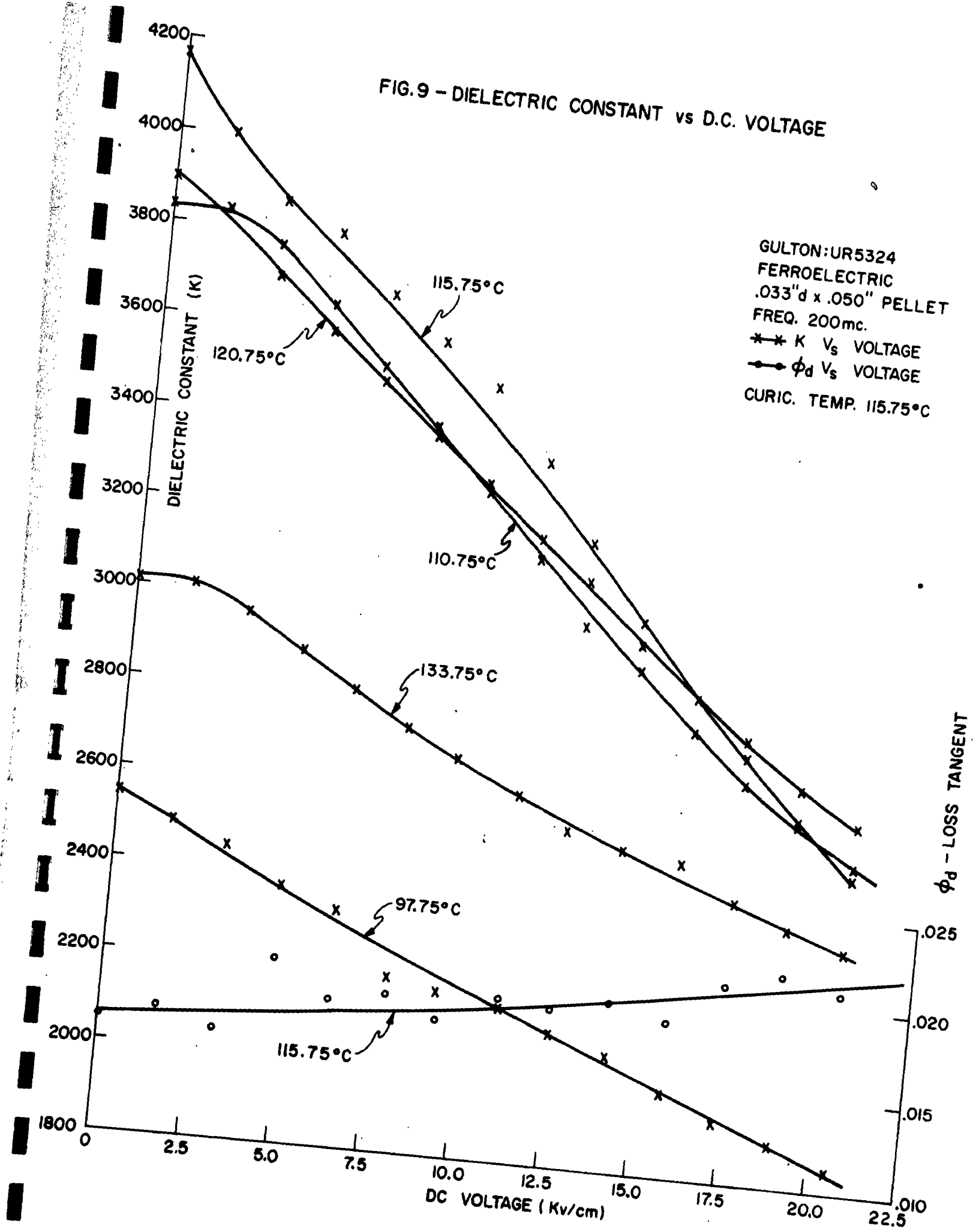


FIG. 9 - DIELECTRIC CONSTANT vs D.C. VOLTAGE



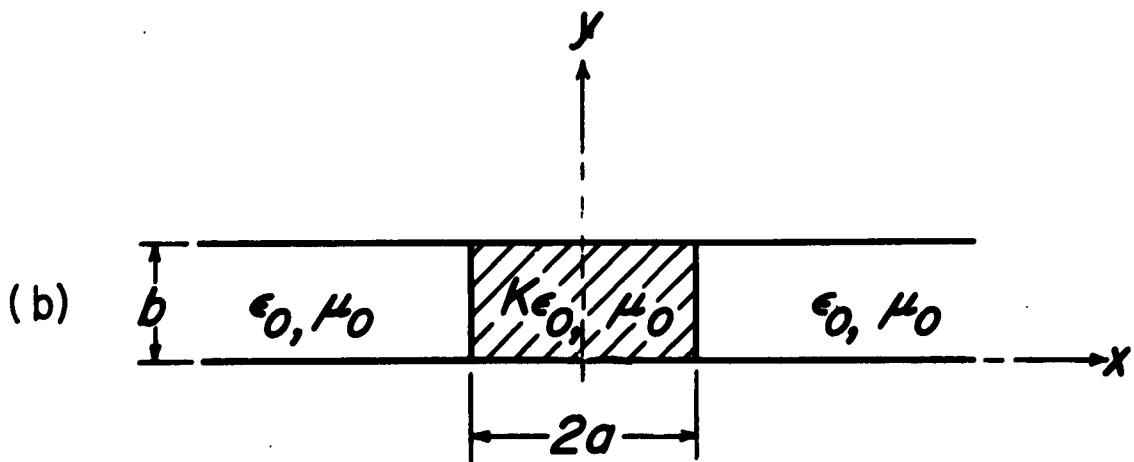
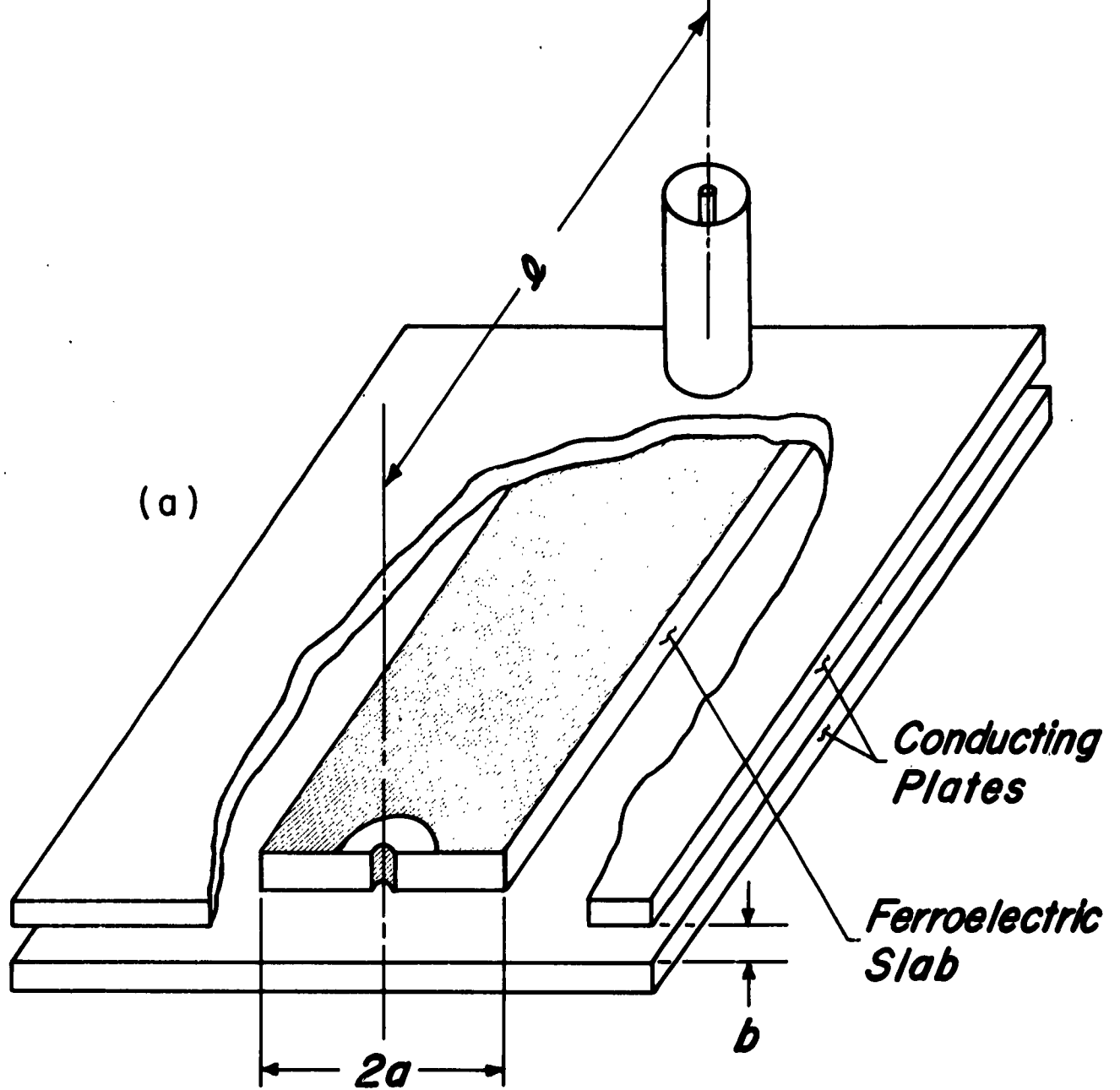


FIG.10- (a) CUTAWAY VIEW OF THE FERROELECTRIC LOADED PARALLEL-PLANE TRANSMISSION LINE (b) CROSS-SECTIONAL VIEW OF THE PARTIALLY DIELECTRIC LOADED PARALLEL PLANE TRANSMISSION LINE.

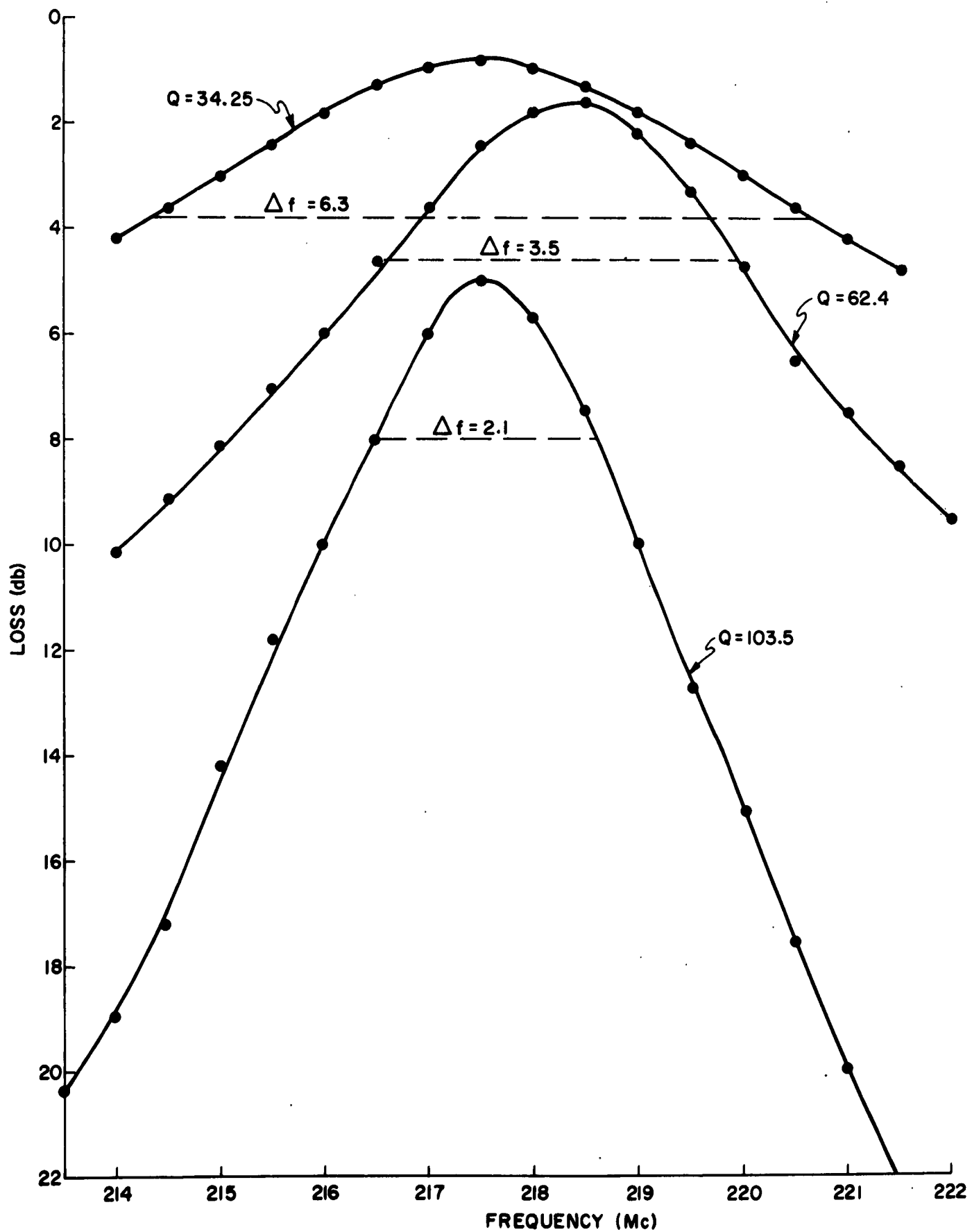
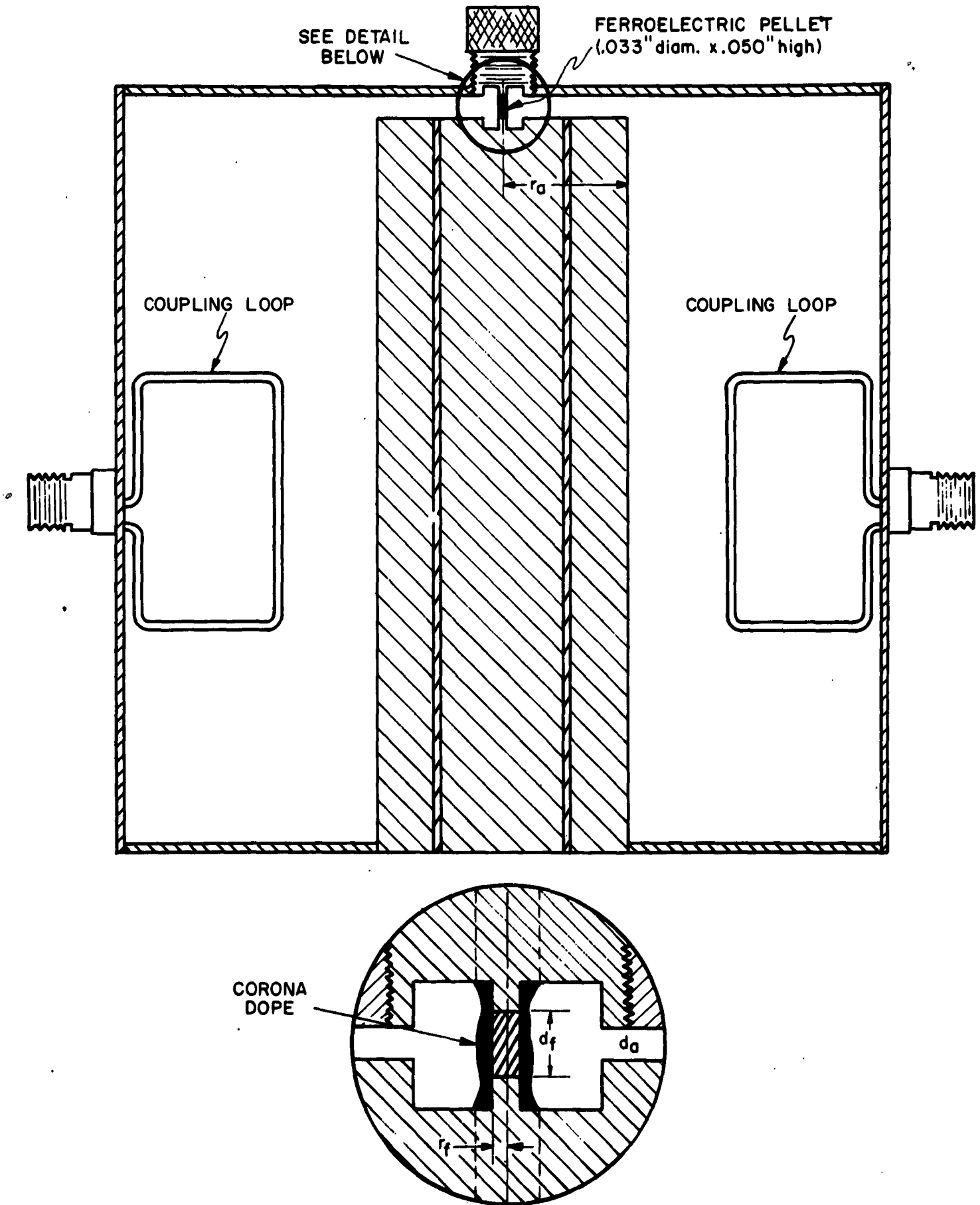


FIG.11 - FREQUENCY RESPONSE OF FERROELECTRIC LOADED CAVITY

FIG. 12 - FERROELECTRIC LIMITER CONFIGURATION



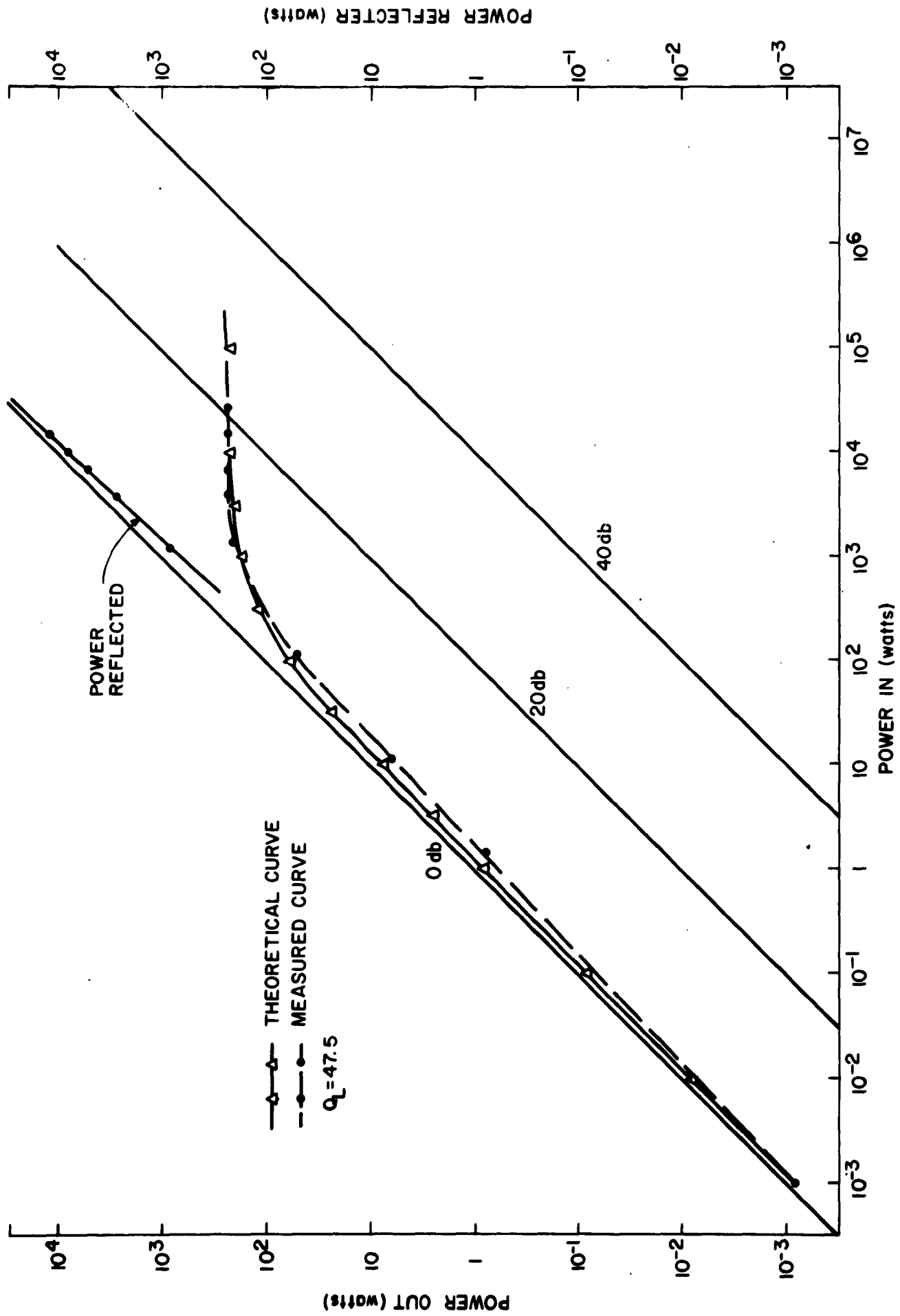


FIG. 13 - FERROELECTRIC LIMITER CHARACTERISTICS

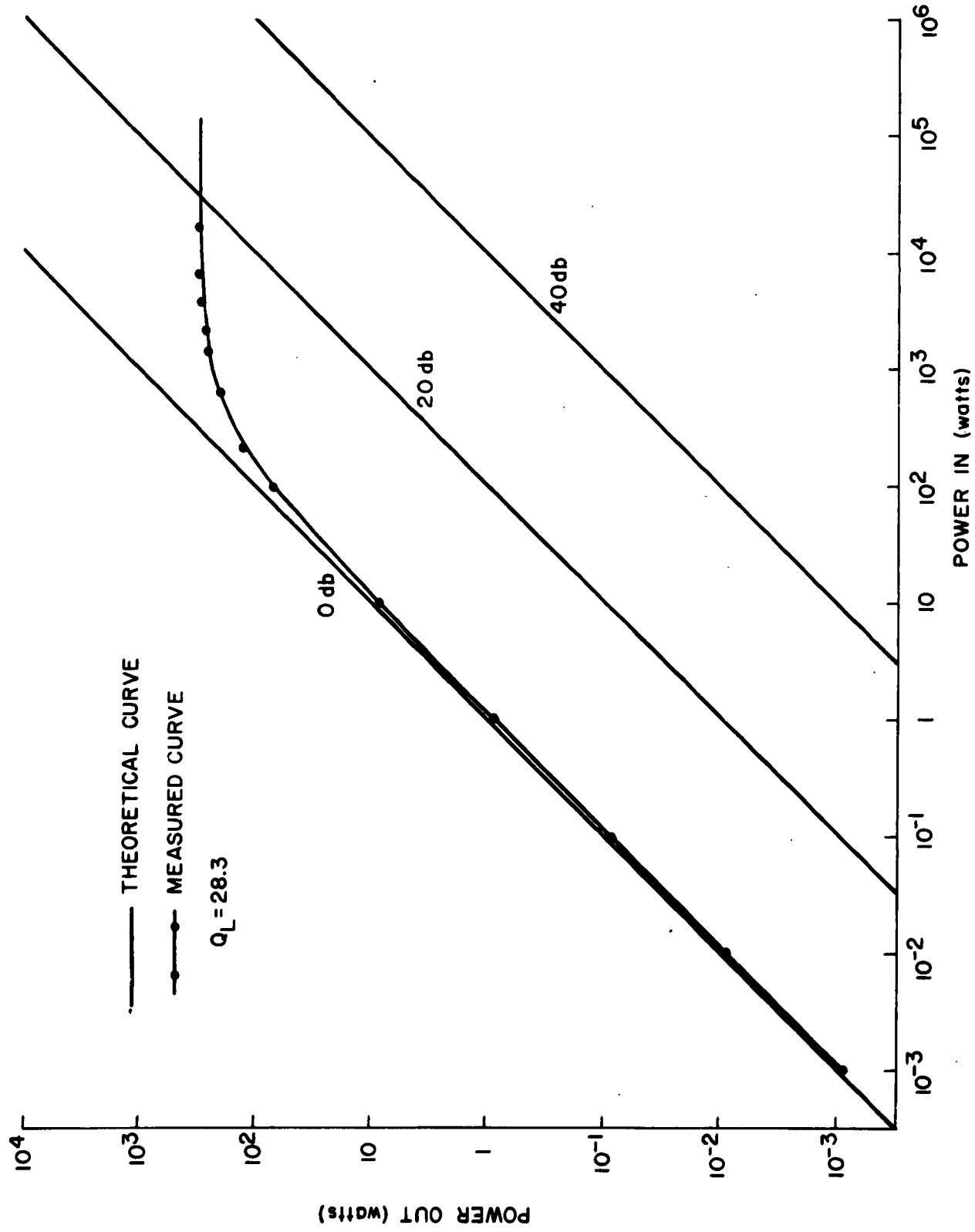


FIG. 14 - FERROELECTRIC LIMITER CHARACTERISTICS

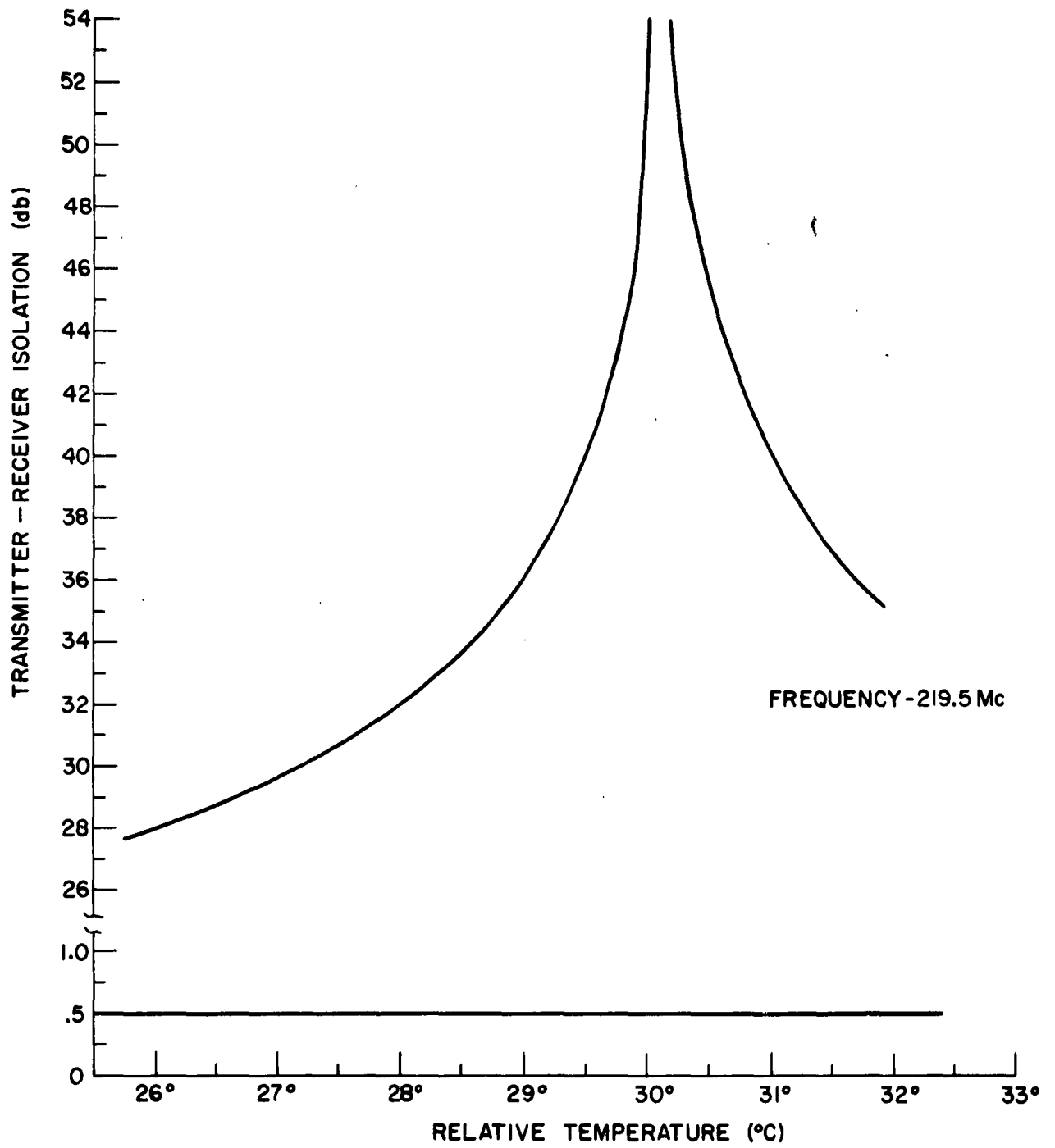


FIG. 15 - PROTOTYPE HIGH POWER CIRCULATOR - LOW POWER CHARACTERISTICS.

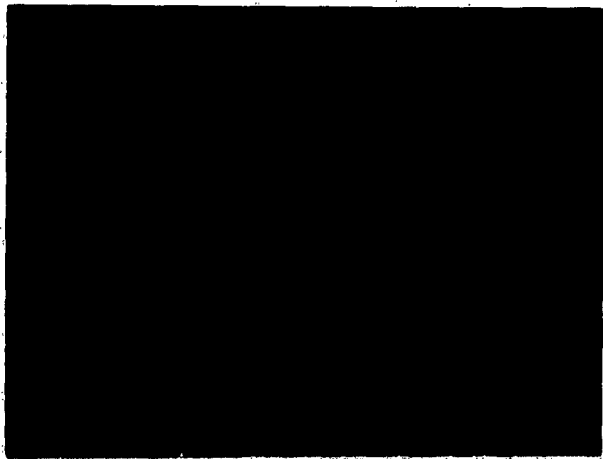


FIG. 16

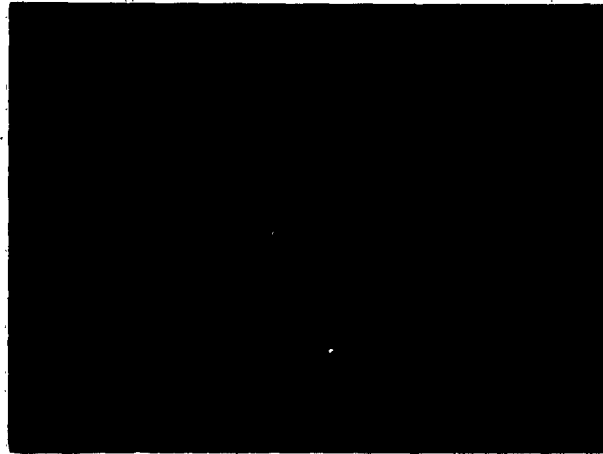


FIG. 17

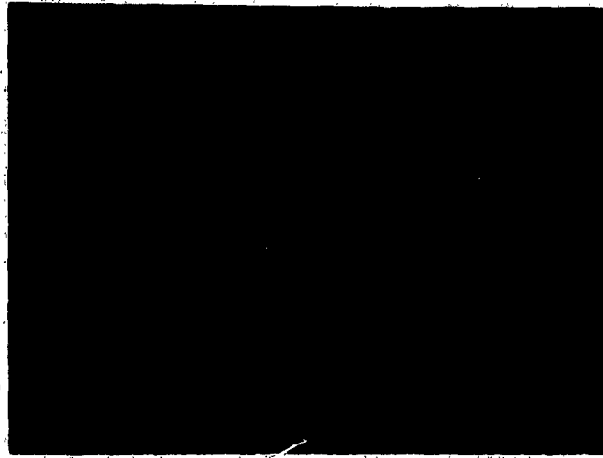


FIG. 18